

# REACTIONS AT SURFACES: FROM ATOMS TO COMPLEXITY

Nobel Lecture, December 8, 2007

by

GERHARD ERTL

Fritz-Haber-Institut der Max-Planck-Gesellschaft, Abteilung Physikalische Chemie, Faradayweg 4-6, DE-14195 Berlin, Germany.

## 1. INTRODUCTION

The secretary of the Royal Swedish Academy of Sciences, the famous chemist Jöns Jacob Berzelius, published since 1820 annual review articles on the most significant new developments in his field. Since the early 19<sup>th</sup> century there were observations from several laboratories whereafter certain substances influenced the progress of a chemical reaction without being consumed and hence apparently not being affected by this reaction. For example, Johann Wolfgang Doebereiner, professor of chemistry at the university of Jena, reported in July 1823 to his minister, J. W. Goethe, *“that finely divided platinum powder causes hydrogen gas to reaction with oxygen gas by mere contact to water where-by the platinum itself is not altered”* [1]. In his report published 1835 Berzelius defined this phenomenon as “catalysis”, rather in order to introduce a classification than to offer a possible explanation [2]. Throughout the rest of this century the term catalysis remained heavily debated [3], until around 1900 W. Ostwald proposed its valid definition in terms of the concepts of chemical kinetics: *“A catalyst is a substance which affects the rate of a chemical reaction without being part of its end products”* [4]. In 1909, Ostwald was awarded the Nobel Prize in Chemistry for his contributions to catalysis.

A chemical reaction involves breaking of bonds between atoms and the formation of new ones. This process is associated with transformation of energy and the energy diagram illustrating the progress of a reaction  $A+B\rightarrow C$  is depicted schematically in fig. 1. The activation energy  $E^*$  to be surmounted is usually provided by thermal energy  $kT$ , with  $k$  being Boltzmann’s constant and  $T$  the temperature, and accordingly not all molecular encounters will be successful, but only a fraction  $e^{-E^*/kT}$ . An increase of the reaction probability (=rate) can be achieved by either increasing the temperature or by lowering the activation energy  $E^*$ . The latter is provided by the catalyst which through the formation of intermediate compounds with the molecules involved in the reaction provides an alternate reaction path as sketched by the dashed line in fig. 1 which is associated with smaller activation barriers and hence a higher

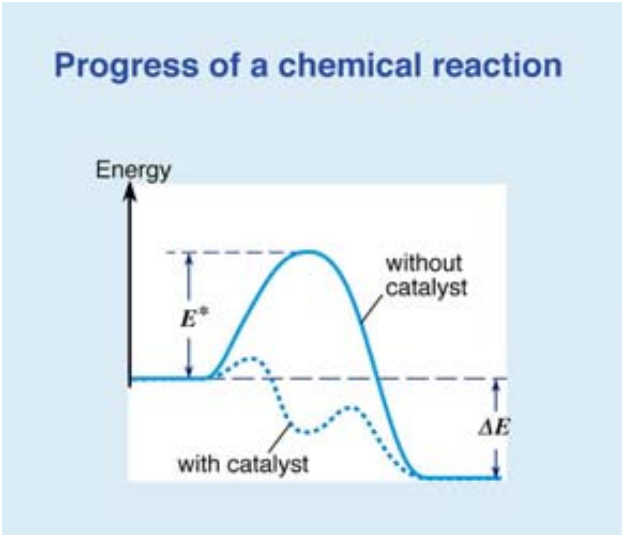


Figure 1. Energy diagram illustrating the progress of a chemical reaction with and without a catalyst.

overall reaction rate. In the last step the product molecules are released from the catalyst which now is available for the next reaction cycle. If the reacting molecules and the catalyst are in the same (gaseous or liquid) phase the effect is called homogeneous catalysis. In living systems macromolecules (=enzymes) play the role of catalysts. In technical reactions mostly the interaction of molecules with the surface of a solid is decisive. The principle of this heterogeneous catalysis is depicted schematically in fig. 2.

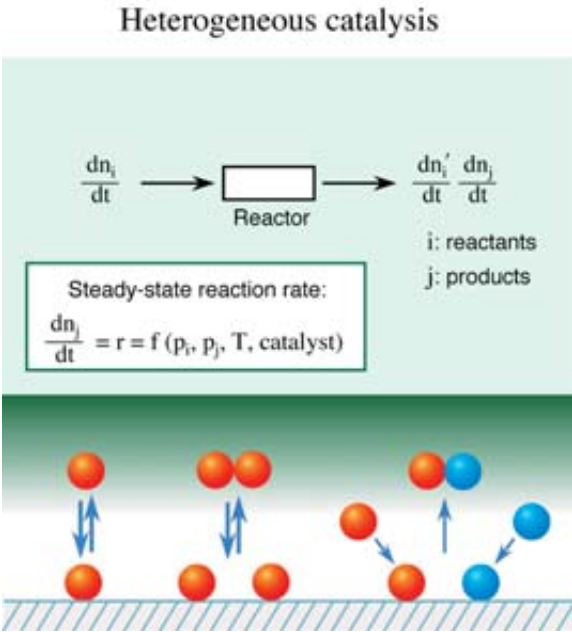


Figure 2. Principle of heterogeneous catalysis.

The atoms in the surface layer of a solid have fewer neighbours than those in the bulk and are hence chemically unsaturated and may form new bonds (=chemisorption) with suitable molecules impinging from the adjacent gas or liquid phase. By this step existing bonds will be modified or may even be broken (=dissociative chemisorption). The surface species formed may jump from one site to neighbouring ones, then may react with others, and the formed produced molecules eventually leave the surface (=desorption). If operated in a flow reactor, the catalyst can in this way continuously operate without being consumed.

One of the first and still most important technical applications of this principle was realized about 100 years ago: Due to the continuous increase of the world population and the exhaust of the natural supply of nitrogen fertilizers the world was facing a global threat of starvation. As Sir William Crookes, president of the British Association for the advancement of sciences, formulated it [8]: “... all civilized nations stand in deadly peril of not having enough to eat. ... the fixation of atmospheric nitrogen is one of the great discoveries awaiting the ingenuity of chemists”.

Nitrogen fixation means transformation of the abundant  $N_2$  molecule (which constitutes about 80% of our air) from its state of very strong bond between the two N atoms into a more reactive form according to the reaction  $N_2 + 3H_2 \rightarrow 2NH_3$ . This reaction of ammonia formation could be realized in 1909 by F. Haber (Nobel Prize 1919) in the laboratory by the use of an osmium catalyst in a high pressure flow apparatus [6]. C. Bosch (Nobel Prize 1931) from the BASF company started immediately to transform this process into technical scale, and the first industrial plant started operation in 1913, only a few years later. Fig. 3 shows the growth of the world population together with the ammonia production over the last century [7], and it is quite obvious that our present life would be quite different without the development of the Haber-Bosch process.

### World population and ammonia production

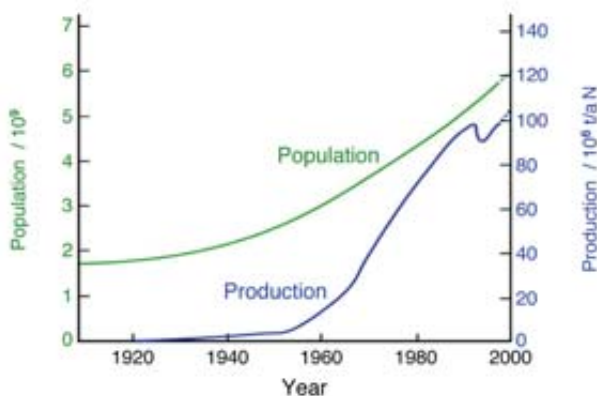


Figure 3. Variation of the world population and the ammonia production during the 20<sup>th</sup> century [7].

However, large scale technical production would not have been possible without the availability of large quantities of a cheap catalyst. (The whole world supply of the precious metal osmium was only 80 kg in those days.) This task could be solved successfully by A. Mittasch [8] who in thousands of tests found that a material derived from a Swedish iron ore exhibited satisfactory activity. This type of doubly-promoted iron catalyst is in fact still in use today in almost all industrial plants.

Remarkably, despite the enormous technical significance of the Haber-Bosch reaction and despite of numerous laboratory studies its actual mechanism remained unclear over many years. P. H. Emmett, one of the pioneers of catalysis research, was honoured in 1974 by a symposium where he concluded at the end [9]: *“The experimental work of the past 50 years leads to the conclusion that the rate-limiting step in ammonia synthesis over iron catalysts is the chemisorption of nitrogen. The question as to whether the nitrogen species involved is molecular or atomic is still not conclusively resolved ...”*.

## 2. THE SURFACE SCIENCE APPROACH TO HETEROGENEOUS CATALYSIS: AMMONIA SYNTHESIS

The problem involved in the study of the surface chemistry of ‘real’ catalysts becomes evident if we look on an electron micrograph of the Mittasch catalyst as reproduced in fig. 4 [10]: A catalyst with high activity has to exhibit a rather high specific surface area which in this case is about 20 m<sup>2</sup>/g as reflected by nanometer sized active particles. (In fact catalysis has been a nanotechnology long before this term was introduced). Under reaction conditions these are reduced into metallic iron covered by a submonolayer of K(+O) which acts as ‘electronic’ promoter. The configuration of active particles is stabilized against sintering by a framework of Al<sub>2</sub>O<sub>3</sub> (and CaO) which compounds act as ‘structural’ promoters. The active component itself will expose different crystal planes apart from various defects, and all these various structural parameters are expected to exhibit varying reactivity. Apart from that, how can the two-dimensional chemistry taking place in the chemisorbed overlayer be investigated down to the atomic scale?

A possible strategy to overcome this problem had been suggested by I. Langmuir (Nobel Prize 1932) already many years ago [11]: *“Most finely divided catalysts must have structures of great complexity. In order to simplify our theoretical consideration of reactions at surfaces, let us confine our attention to reactions on plane surfaces. If the principles in this case are well understood, it should then be possible to extend the theory to the case of porous bodies. In general, we should look upon the surface as consisting of a checkerboard ...”*

The ‘surface science’ approach which Langmuir had in mind was experimentally not yet accessible in his days, but began to become only available during the 1960’s with the advent of ultrahigh vacuum (UHV) and surface sensitive physical methods [12]. Nowadays a whole arsenal of such techniques is available to study the structural, electronic or dynamic properties of such well-defined single crystal surfaces.

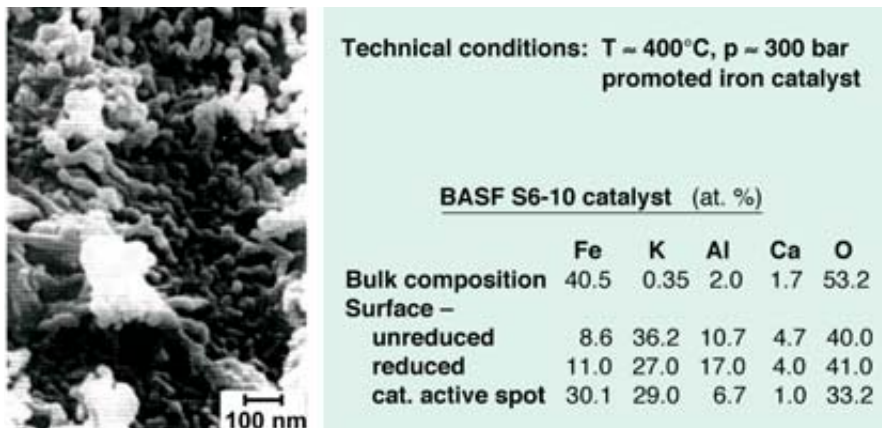


Figure 4. Surface topography and chemical composition of an industrial ammonia synthesis catalyst [10].

Bond-breaking upon chemisorption is perhaps the most important role of a catalyst. Fig. 5 shows schematically the energetic transformations in such a process if a diatomic molecule interacts with a perfect surface. Upon approaching the surface the molecule may initiate the formation of new bonds to the surface atoms whereby the bond between the two atoms is weakened. A corresponding one-dimensional energy diagram as proposed by Lennard-Jones [15] is depicted in fig. 5a: If the molecule  $A_2$  forms a bond with the surface a shallow minimum ( $A_{2,ad}$ ) is reached. If instead the free  $A_2$  molecule dissociated the dissociation energy  $E_{diss}$  is needed. Chemisorption of two A atoms would be associated with strong bond formation ( $2A_{ad}$ ), and the crossing point between the two curves obviously marks the activation energy for dissociative chemisorption, viz.  $A_2 \rightarrow 2A_{ad}$ . Even more instructive is a two-dimensional diagram (fig. 5b), where lines of equal energy are plotted as a function of the distance  $x$  between the molecule and the surface and the separation  $y$  between the two atoms. (A full multi-dimensional description would require knowledge of the energy also as function of the point of impact within the unit cell of the surface as well as of the orientation of the molecular axis, and theory is nowadays able to provide this information as well as on the dynamics of energy transfer between the different degrees of freedom [14].)

Fig. 6 shows a scanning tunneling microscope (STM) picture from a Pt(111) surface with atomic resolution after exposure to a small amount of  $O_2$  molecules at 165 K [15]. Apart from the Pt atoms from the topmost layer additional features, namely pairs of bright dots surrounded by dark rings are visible. The dots mark the positions of O atoms resulting from dissociative chemisorption. While at 120 K instead chemisorbed  $O_2$  molecules would be discernible, at 165 K the thermal energy suffices to overcome the activation barrier for dissociation. The dark rings around the bright spots reflect the modification of the local electronic structure near the chemisorbed species. As a consequence neighboring particles interact with each other through the electronic system of the substrate, whereby these interactions may be repul-

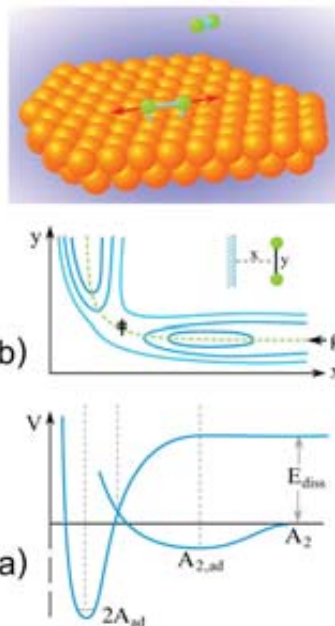


Figure 5. Energy diagram illustrating the process of dissociative chemisorption of a diatomic molecule: a) One-dimensional Lennard-Jones diagram. b) Two-dimensional representation of equipotential lines as function of the distance  $x$  of the molecule from the surface and the separation  $y$  between the two atoms.

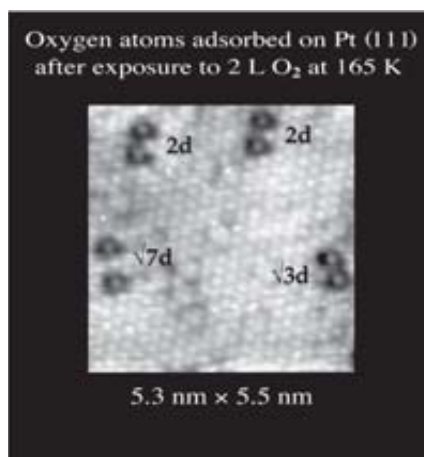


Figure 6. Scanning tunneling microscope (STM) image from a Pt(111) surface after exposure of a small concentration of  $O_2$  molecules at 165 K [15].

sive as well as attractive [18]. At the low temperature of 165 K, on the other hand, the chemisorbed O atoms are immobile and rest at those sites at which transfer of the chemisorption energy to the solid has been completed. This process requires a certain relaxation time during which the two separating O atoms move apart from each other. That is why two O atoms are never on neighboring sites, but are typically separated by 0.5 – 0.8 nm from each other. Taking into account the chemisorption energy released leads to an estimate of about  $3 \times 10^{-13}$  s for the lifetime of these ‘hot’ adsorbed atoms.

More detailed insight into the dynamics of energy exchange between the solid and chemisorbed species can be obtained by application of ultrafast (femtosecond) laser techniques, and it can be generally concluded that with metal surfaces complete thermal equilibrium between all degrees of freedom is typically reached after about  $10^{-12}$  s [17].

The mean residence time of a chemisorbed particle on its momentary adsorption site is given by  $\tau = \tau_0 e^{E_{\text{diff}}^*/kT}$  whereby  $E_{\text{diff}}^*$  is the activation energy for surface diffusion to a neighboring site. ( $E_{\text{diff}}^*$  is always much smaller than the adsorption energy, so that the adsorbed particles makes many jumps before it eventually desorbs into the gas phase.) Fig. 7a shows a snapshot taken with a fast STM from a Ru(001) surface at 300 K covered by a small concentration of O atoms. The latter jump around like with two-dimensional Brownian motion with a mean  $\tau$  of about  $6 \times 10^{-2}$  s. However,  $\tau$  varies with the mutual separation between two neighboring O atoms due to the operation of the above mentioned interactions and reaches about 0.22 s if the two O atoms are separated from each other by 2 lattice constants [19]. As a consequence of the operation of these weak attractive interactions at higher surface concentrations the adsorbed particles are no longer uniformly and randomly distributed across the surface, but segregate into two phases as shown in fig. 7b: A two-dimensional quasi-solid phase is in equilibrium with a quasi-gas phase, where continuous nucleation, condensation and sublimation occur like in analogous solid-gas equilibria. From such observations it becomes also obvious that definition of a surface diffusion coefficient for adsorbates is meaningful only at low surface concentrations as long as the adsorbed particles can be considered to be independent from each other [20].

The formation of ordered adsorbate phases with long-range periodicity like in fig. 7b is quite common and permits determination of the actual structural parameters by a diffraction technique, preferably low energy electron diffraction (LEED) [12]. If we now return to the original problem of ammonia synthesis, dissociative chemisorption of nitrogen on various Fe single crystal surfaces causes indeed also the formation of such structures derived from chemisorbed N atoms, such as reproduced in fig. 8 for the  $c2 \times 2$ -N phase on the Fe(100) surface [21]. The probability for this process (=sticking coefficient) is very low, typically of the order  $10^{-6}$ , which reflects the fact that this step is indeed rate-limiting in the overall reaction of ammonia synthesis. Fig. 9 shows the variation of the surface concentration  $\gamma$  (in relative units) of N atoms chemisorbed on various Fe single crystal surfaces with exposure (i.e. number of molecules impinging per  $\text{cm}^2$  and s) to  $\text{N}_2$  gas at  $T = 693$  K [22].



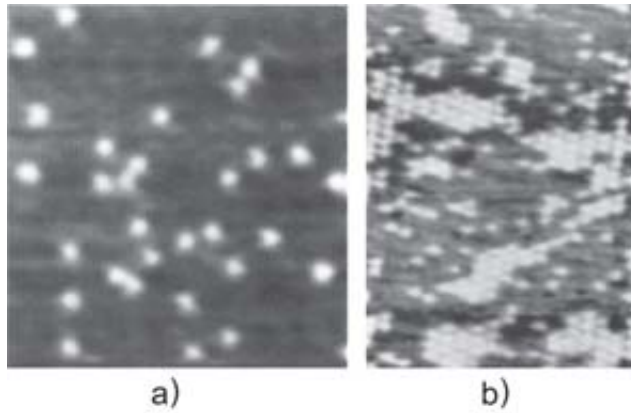


Figure 7. STM snapshots from O atoms adsorbed on a Ru(001) surface at  $T = 300$  K [18]. a) very small coverage. b) higher coverage. In the lecture a short movie was presented showing the motion of the O atoms in real time.

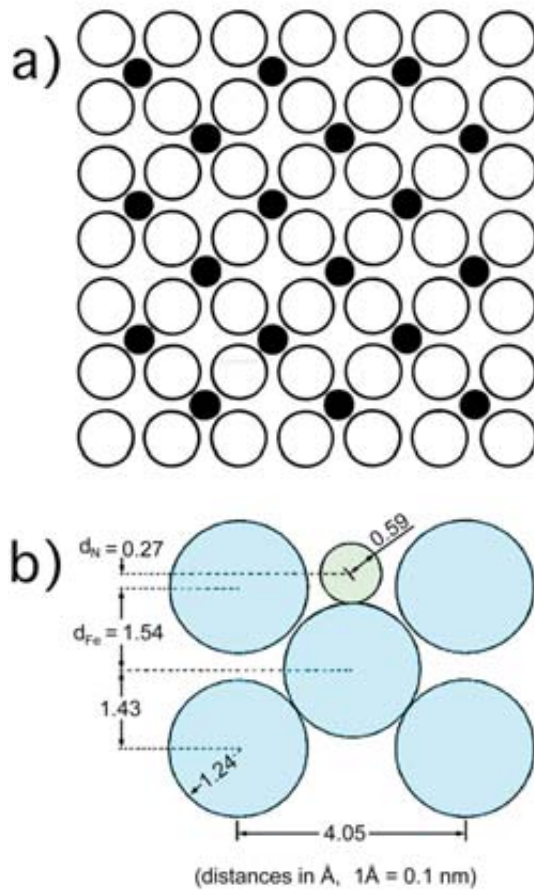


Figure 8. The structure of N atoms chemisorbed on a Fe(100) surface [21]. a) top view b) side view.



Figure 1 is a line graph showing the dependence of surface energy  $\gamma$  (in J/m<sup>2</sup>) on N<sub>2</sub> exposure (in units of 10<sup>7</sup> L) for Fe(100) and Fe(110) surfaces at T = 693 K. The y-axis represents  $\gamma$  and ranges from 0 to 7. The x-axis represents N<sub>2</sub> exposure and ranges from 0 to 9. There are three curves: Fe(111) (top), Fe(100), T = 693 K (middle), and Fe(110) (bottom). The Fe(111) curve starts at approximately 3.8 J/m<sup>2</sup> and increases to about 5.8 J/m<sup>2</sup>. The Fe(100) curve starts at 0 and increases to about 6.8 J/m<sup>2</sup>. The Fe(110) curve starts at 0 and increases to about 3.0 J/m<sup>2</sup>. To the right of the graph are three diagrams illustrating the atomic structure of the Fe(111), Fe(100), and Fe(110) surfaces. Fe(111) is a hexagonal close-packed layer, Fe(100) is a square close-packed layer, and Fe(110) is a rectangular close-packed layer.

There is a pronounced influence of the surface structure: The most densely packed (110) surface is least active, while the open (111) plane exhibits the highest sticking coefficient and is indeed also responsible for the overall activity of the industrial catalyst [23]. This activity is further enhanced by the presence of the electronic promoter K which stabilizes the intermediate  $\text{N}_{2,\text{ad}}$  complex and hence increases its dissociation probability [24]. The same sequence in reactivity as found for the sticking coefficient for dissociative nitrogen adsorption under low pressure conditions was also found for the yield of ammonia production at 20 bar pressure [25]. Thus it is also demonstrated that in this case there exists no ‘pressure gap’.

Energy level diagram for the nitrogen fixation pathway on a metal surface. The diagram shows the relative energies of various species in kJ/mol. The reference level is N + 3H at 1400 kJ/mol. Other species include 1/2 N<sub>2</sub> (1129 kJ/mol), 1/2 N<sub>2ad</sub> (17 kJ/mol), 3/2 H<sub>2</sub> (259 kJ/mol), 3/2 H<sub>2ad</sub> (106 kJ/mol), NH (314 kJ/mol), NH<sub>2</sub> (389 kJ/mol), NH<sub>ad</sub> (543 kJ/mol), NH<sub>2ad</sub> (501 kJ/mol), and NH<sub>3</sub> (460 kJ/mol). The activation energy for the final step (NH<sub>2ad</sub> + H<sub>ad</sub> to NH<sub>3</sub>) is 46 kJ/mol.

Chemical reactions shown:

$$\text{N}_2 \rightleftharpoons \text{N}_{2ad} \rightleftharpoons 2\text{N}_{ad}$$

$$\text{H}_2 \rightleftharpoons 2\text{H}_{ad}$$

$$\text{N}_{ad} + \text{H}_{ad} \rightleftharpoons \text{NH}_{ad}$$

$$\text{NH}_{ad} + \text{H}_{ad} \rightleftharpoons \text{NH}_{2ad}$$

$$\text{NH}_{2ad} + \text{H}_{ad} \rightleftharpoons \text{NH}_{3ad} \rightleftharpoons \text{NH}_3$$

124

All further steps involved in the ammonia synthesis reaction could be identified and analyzed similarly, so that the overall mechanism and energy diagram reproduced in fig. 10 could be derived [26]. This diagram exhibits the general features of the schematic diagram of fig. 1: Instead of overcoming the prohibitive high energy barrier for dissociation of the reacting molecules the catalyst offers an alternate reaction path through formation of intermediate chemisorption complexes whose energy differences can be readily surmounted by the available thermal energy.

The kinetic parameters associated with the individual reaction steps can be put together to calculate the steady-state yield of ammonia formation for given external parameters. Fig. 11 shows a plot of the ammonia yield derived on the basis of this kinetic model as a function of the experimental yields in industrial plants [27]. The data points barely deviate from the straight line which marks complete agreement between theory and experiment. This result could be confirmed also by others [28] and demonstrates that in this case the 'surface science' approach is indeed able to lead even to a quantitative description of an industrial reaction of great relevance.

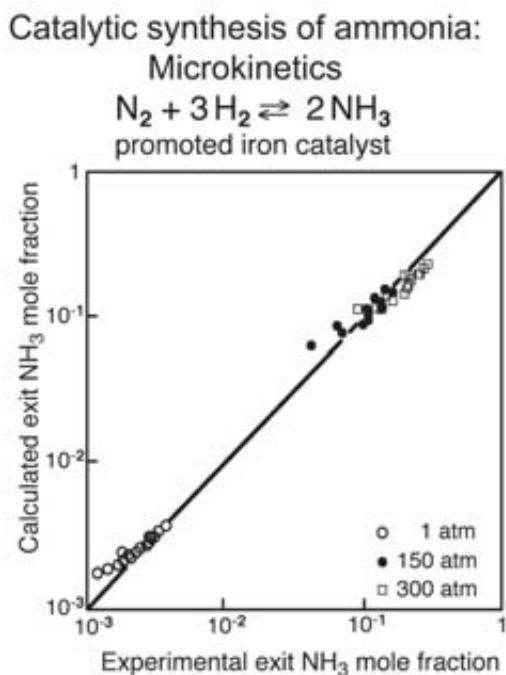


Figure 11. Microkinetics of catalytic ammonia synthesis. Comparison of the yield calculated on the basis of the mechanism presented in Figure 10 with experimental data from industrial plants [27].

### 3. SELF-ORGANISATION AND COMPLEXITY: OXIDATION OF CARBON MONOXIDE

One of the major applications of heterogeneous catalysis in our days concerns protection of the environment through removal of toxic substances from car exhausts. Oxidation of carbon monoxide to carbon dioxide,  $2\text{CO} + \text{O}_2 \rightarrow 2\text{CO}_2$ , is the simplest of these reactions and is depicted schematically in fig. 12. The exhaust gas flows through the catalytic converter where the molecules interact with the surfaces of finely divided metal particles from the platinum group. Thereby the  $\text{O}_2$  molecules are dissociatively chemisorbed, and the formed  $\text{O}_{\text{ad}}$  species interact with chemisorbed CO molecules to  $\text{CO}_2$  which is immediately released into the gas phase.

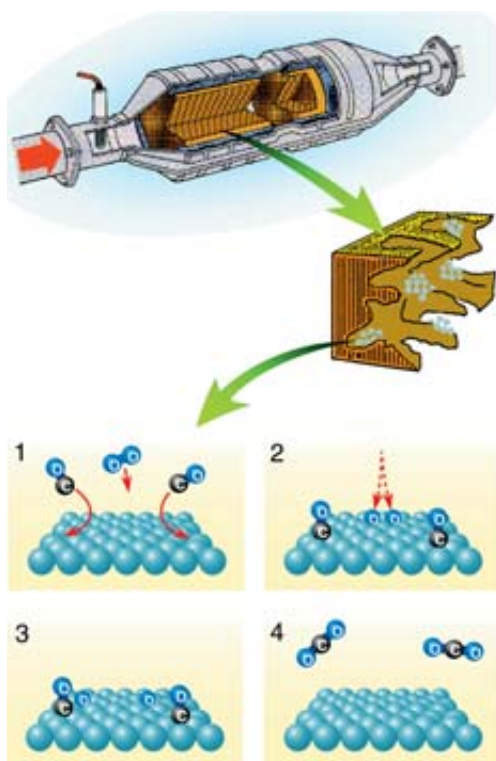


Figure 12. Cartoon illustrating a car exhaust catalyst and the mechanism of CO oxidation.

The structures formed by chemisorbed O and CO on a Rh(111) surface as example are shown in fig. 13 [29]: The CO molecules are in this case bonded through the C atom in 'on top' positions. They exhibit always the tendency for the formation of densely packed layers, eventually even with occupancy of different adsorption sites [30] (fig. 13a). The O atoms, on the other hand, occupy threefold-coordinated sites and form a rather open mesh of a  $2 \times 2$ -structure (fig. 13b). Since an  $\text{O}_2$  molecule in order to become dissociated requires an ensemble of neighboring empty surface atoms, this process will

be inhibited as soon as the CO coverage exceeds a certain critical value. The open structure of the adsorbed O-layer, on the other hand, still permits adsorption of CO, leading to a mixed phase as reproduced in fig. 13c where the two reactants are in close contact and can readily recombine to CO<sub>2</sub>. Under steady-state flow conditions in a mixture of O<sub>2</sub>+CO the surface of the catalyst will soon be fully covered by adsorbed CO which prevents oxygen adsorption and hence suppresses the reaction. This problem can only be overcome if the temperature is high enough ( $\geq 450$  K) to enable continuous desorption of part of the adsorbed CO so that gaseous O<sub>2</sub> may compete for these free adsorption sites. (This is the reason why the catalyst of your car does not work in the cold but needs a certain minimum temperature.) The sequence of reaction steps and the energy diagram for this reaction is depicted in fig. 14: After chemisorption of the reactants, O<sub>ad</sub>+CO<sub>ad</sub> may recombine according to the Langmuir-Hinshelwood mechanism [31] by overcoming an activation barrier of 100 kJ/mol (which is only about half as high at higher coverages [31]), – a result which could also be confirmed theoretically on the basis of DFT calculations [32].

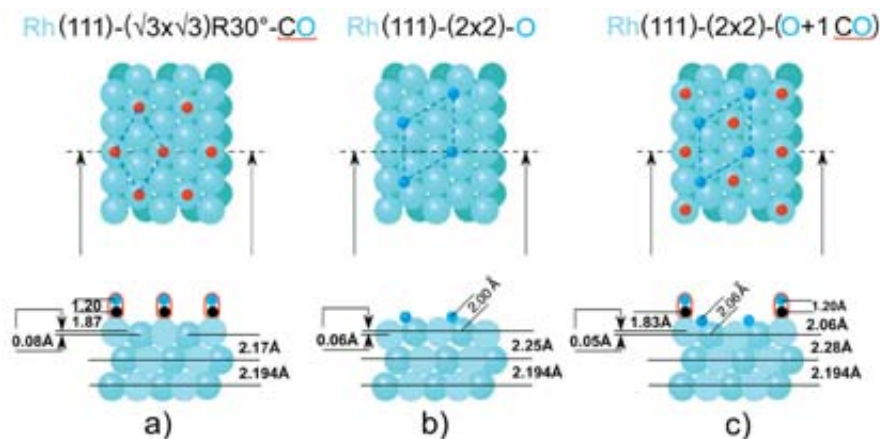


Figure 13. Structures of CO (a), O (b), and O+CO (c) chemisorbed on a Rh(111) surface [29].

Under steady-state flow conditions the rate of product formation will usually be constant and a function of the external parameters temperature and partial pressure of O<sub>2</sub> and CO, – however, with exceptions under rare conditions: Already around 1970, it was found in Wicke's laboratory [33] that with supported Pt catalysts sometimes the rate exhibits temporal oscillations. Such a situation can also be found with a well-defined Pt(110) surface as shown in fig. 15 [34]: At the time marked by an arrow the O<sub>2</sub>-pressure was steplike raised from 2.0 to 2.7x10<sup>-4</sup> mbar. As a consequence the rate slowly increases and then develops periodic variations with finally constant high amplitudes.

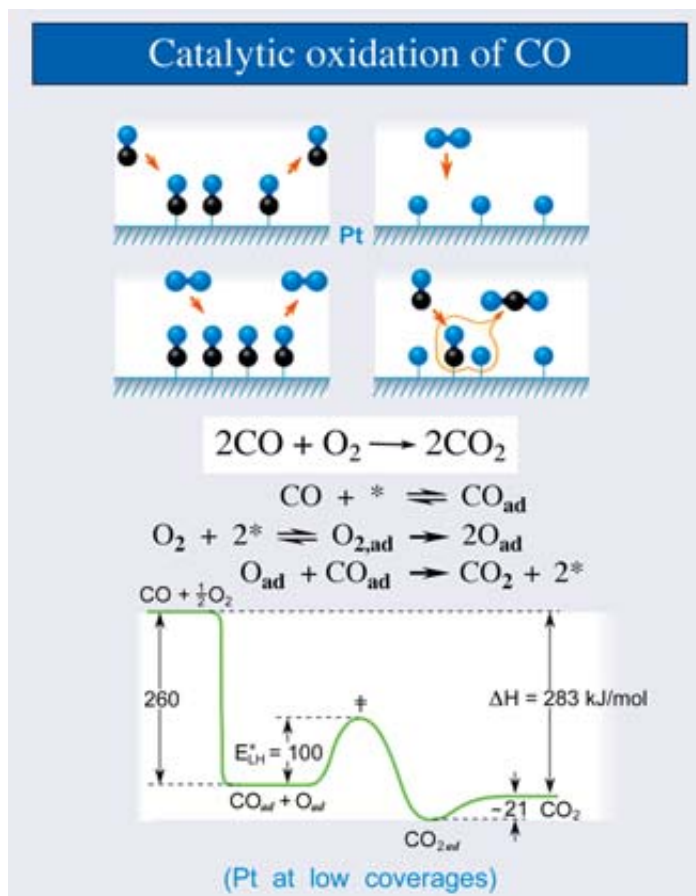


Figure 14. Mechanism and energy diagram for the catalytic oxidation of CO on Pt.

Characteristic for the present system is that it is far away from equilibrium and may develop so-called dissipative structures as explored in detail by Prigogine (Nobel Prize 1977) [35] and by Haken [36] in the framework of synergetics. A particularly spectacular example for such behavior from population dynamics is reproduced in fig. 16 [37] which shows the variation with time of the number of furs from hares and lynxes delivered to Hudson's Bay Company. The oscillating populations of both species are coupled to each other with a certain phase shift. The reason seems to be quite obvious: If the lynxes find enough food (=hares) their population grows, while that of the hares decays as soon as their birth rate cannot compensate their loss any more. When the supply of hares drops, the lynxes begin to starve and their population also decays so that that of the hares can recover. The variations of the populations of the two species  $x$  and  $y$  can be modeled in the language of chemical kinetics in terms of two coupled nonlinear (ordinary) differential equations (Lotka-Volterra model) as shown in fig. 17 together with their solution for properly chosen parameters  $\alpha$  and  $\beta$ . This solution exhibits just the qualitative behavior of the data of fig. 16.

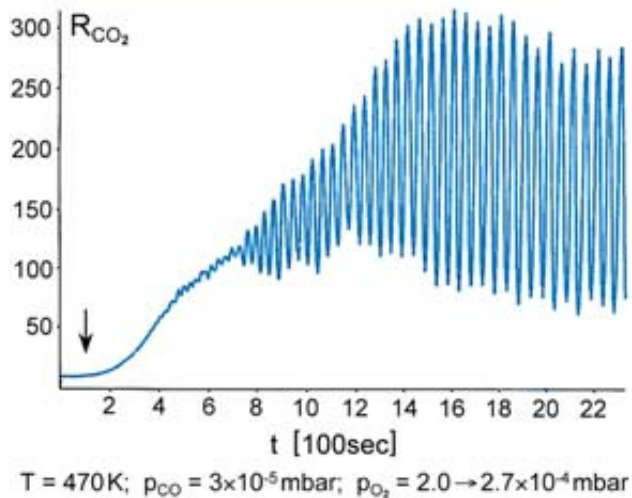


Figure 15. Onset of temporal oscillations of the rate of  $\text{CO}_2$  formation on a  $\text{Pt}(110)$  surface [34].

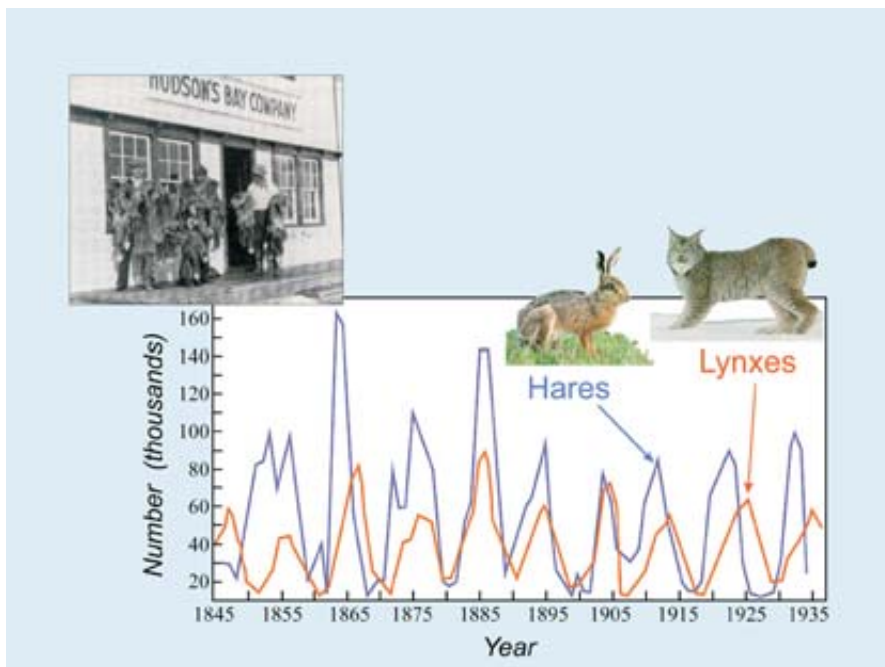


Figure 16. Variation of the number of furs from hares and lynxes delivered to Hudson's Bay company with time [37].



## Lotka-Volterra Model

$$\frac{dx}{dt} = \alpha_1 x - \alpha_2 xy$$

$$\frac{dy}{dt} = \beta_1 xy - \beta_2 y$$

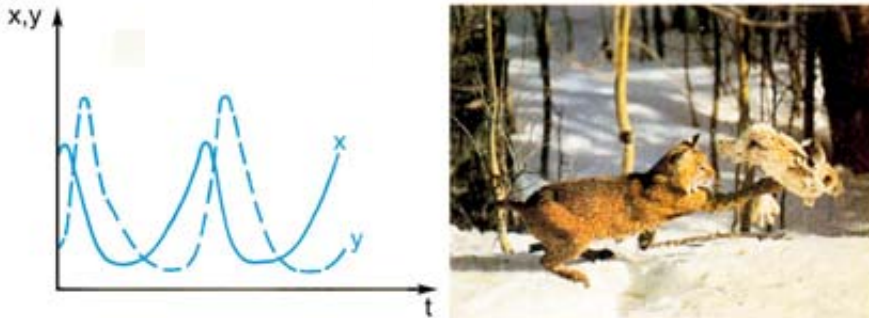


Figure 17. The Lotka-Volterra model.

Mathematical description in terms of nonlinear differential equations is essential for these effects, and therefore this field is also denoted as nonlinear dynamics.

With the oscillatory kinetics in the CO oxidation on Pt(110) the situation is still somewhat more complicated. In this case the reason for this effect has to be primarily sought in the structure of the Pt(110) surface and its transformation under the influence of adsorbates. As already recognized by Langmuir [38]: *“The atoms in the surface of a crystal must tend to arrange themselves so that the total energy will be a minimum. In general, this will involve a shifting of the positions of the atoms with respect to each other.”*

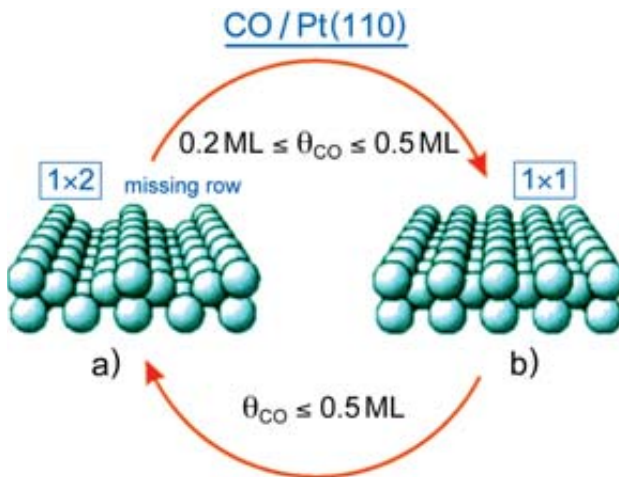


Figure 18. The structure of the Pt(110) surface [39] a) The 1x2-structure of the clean surface, b) the 1x1-structure representing termination of the bulk structure.



Such a reconstruction is exhibited by the clean Pt(110) surface [39]. Instead of the termination by the corresponding bulk crystal plane (fig. 18b = 1x1 structure), every second row along the  $[1\bar{1}0]$  direction is missing, giving rise to as 1x2-structure (fig. 18a). In this way small facets with (111)-orientation are exposed, leading to a lower energy than with the 1x1-phase. The two phases differ also with respect to their adsorption properties: Chemisorption of CO is accompanied by a higher adsorption energy on the 1x1-phase than on the 1x2-structure, so that local 1x2 $\rightarrow$ 1x1 transformation takes place as soon as the CO coverage exceeds a value of 0.2 monolayers (ML) [40]. On the other hand, the sticking coefficient for dissociative oxygen coverage on the 1x1-phase exceeds that on the 1x2-phase by about 50% [41]. The occurrence of temporal oscillations in the rate of CO<sub>2</sub> can now be rationalized as follows: If a clean Pt(110) surface (1x2) is exposed to a proper mixture of CO+O<sub>2</sub>, adsorption of CO will suffice to cause local 1x2 $\rightarrow$ 1x1 transformation. On the newly created 1x1-patches, the oxygen sticking coefficient will be higher, so that a higher O coverage will be built up, giving rise to an enhanced production of CO<sub>2</sub>. By this latter process the excess CO will be consumed so that the surface structure transforms back from 1x1 $\rightarrow$ 1x2, and one cycle is completed. Mathematical modeling requires in this case three variables, the coverages of O and CO, and the fraction of the surface being present as 1x1-phase. Solution of the resulting 3 coupled nonlinear differential equations for properly chosen parameters is shown in fig. 19 and reproduces the experimental findings [42].

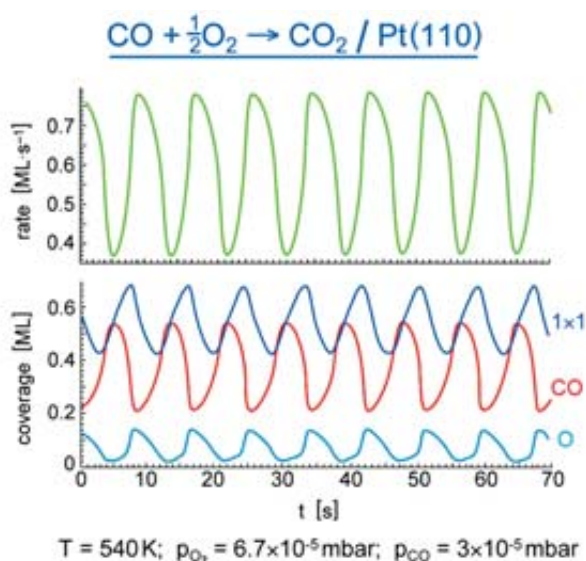


Figure 19. Theoretical description of the oscillatory kinetics of CO oxidation on a Pt(110) surface [42].

However, so far the story is still incomplete: If the elements of an extended system exhibit temporal oscillations as a whole, some kind of lateral coupling between these elements is required in order to achieve synchronization. As a consequence of these considerations the state variables (i.e. the surface concentrations of the adsorbates  $x_i$ ) are in general not only depending on time  $t$  but also on the spatial coordinates  $r_i$ . As summarized in fig. 20 coupling between different regions on the surface is achieved by transport processes. If the heat capacity of the catalyst is low enough, spots with surface concentrations favouring higher reaction rates will also attain higher local temperature due to the exothermicity of the overall reaction, and then heat conduction across the catalyst surface will provide coupling between different parts. Such a situation will usually be found with oscillatory kinetics on supported catalysts under high pressure conditions [43], but has also been studied in detail with a very thin ( $\sim 200$  nm) Pt(110) single crystal foil, where periodic variation of the reaction rate caused corresponding changes of the temperature. The latter effect initiated varying thermal expansion and hence deformation which was denoted as ‘heartbeats of a catalyst’ [44].

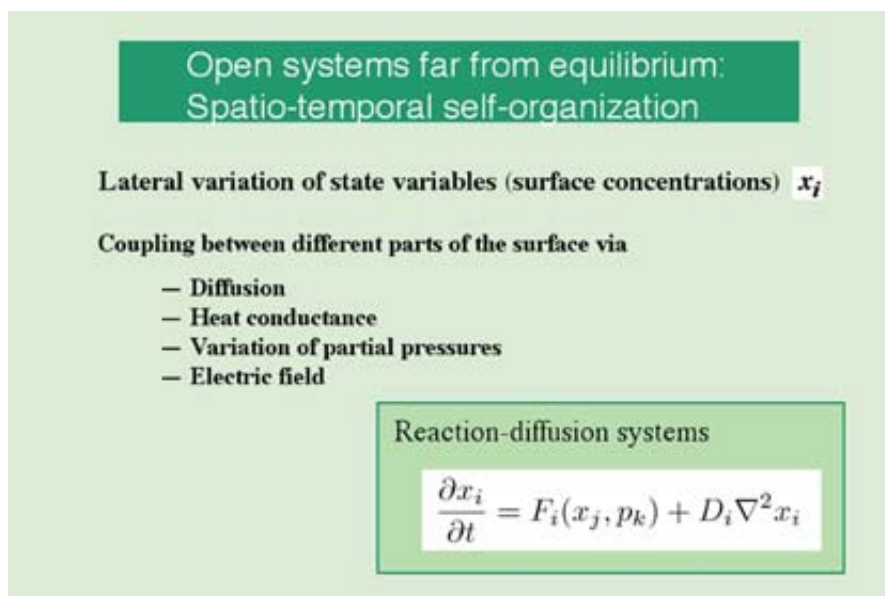


Figure 20. Spatio-temporal self-organisation in open systems far from equilibrium.

Under isothermal conditions at low pressures local differences of the surface concentrations cause surface diffusion of the adsorbates, and mathematical description can now be obtained in terms of reaction-diffusion equations, i.e. a set of coupled nonlinear partial differential equations combining the kinetics with the diffusion of the adsorbed species (fig. 20). The length scale of the resulting spatio-temporal concentration patterns is no longer governed by atomic dimensions but by the so-called diffusion length, which in our case is of the order of tens of microns [45]. These patterns were

imaged by the technique of photoemission electron microscopy (PEEM) [46]: Adsorbed O and CO species are accompanied by different electric dipole moments and hence different work function changes which in turn give rise to varying intensities of photoemitted electrons. In the images to be shown dark areas are essentially O-covered while brighter patches are CO-covered. As an example fig. 21 shows so-called target patterns, concentric elliptic features propagating preferentially along the  $[\bar{1}\bar{1}0]$ -direction of the Pt(110) surface (where CO diffusion is faster than along the  $[001]$ -direction) on a background changing periodically between bright (=CO covered) and dark (=O covered), while the external parameters of temperature and partial pressures are kept constant as indicated [47].

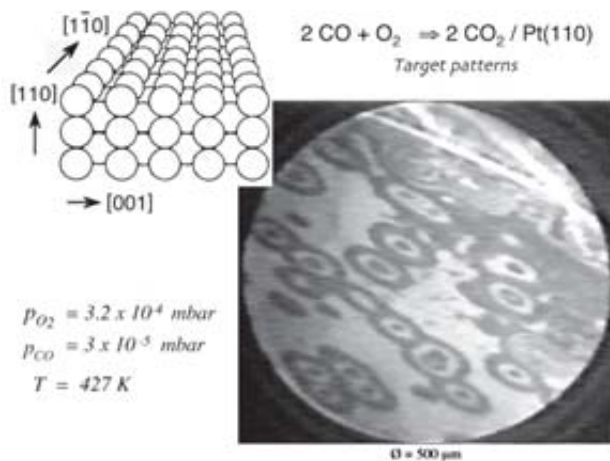


Figure 21. Target patterns in catalytic oxidation of CO on a Pt(110) surface as imaged by photoemission electron microscopy (PEEM) [47]. Here as well as with figs. 22 and 25 again real-time movies were presented.

Under other external parameters typical spiral waves as shown in fig. 22 develop and propagate with front speeds of a few  $\mu\text{m/s}$ . The core of a spiral is often formed by a region on the surface with enhanced defect density, and this effect is also responsible for the fact that the wavelengths of the spiral vary to some extent [48].

## Spiral waves during CO-oxidation on Pt(110)



PEEM images with 500  $\mu\text{m}$  diameter,  
steady-state conditions:  $p_{\text{O}_2} = 4 \times 10^{-4}$  mbar,  $p_{\text{CO}} = 4.3 \times 10^{-5}$  mbar,  $T = 448$  K

Figure 22. PEEM image from the formation of spiral-waves in catalytic CO oxidation on a Pt(110) surface [48].

Since the mechanism of this reaction and all its parameters are well established experimentally, these data may also be used to simulate the resulting patterns by numerical solution of the underlying differential equations. This is shown in fig. 23 for the case of spiral wave development [49]. If the parameters are slightly changed, the solution exhibits no longer regular spirals, but they break-up to the situation of spiral-turbulence or spatio-temporal chaos (fig. 24). Experimental verification of such a situation is demonstrated by fig. 25.

### *Computer simulation: Spiral formation*

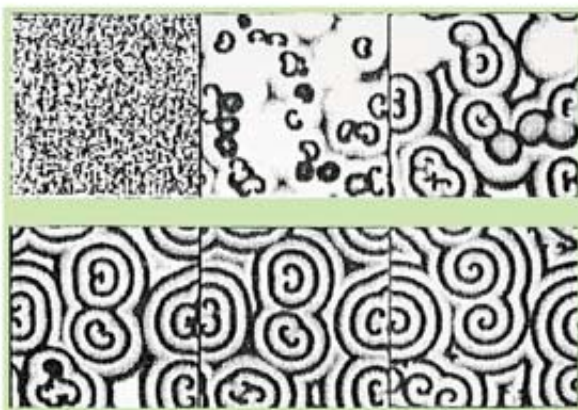


Figure 23. Computer simulation of the evolution of spiral waves in catalytic CO oxidation [49].

## Computer simulation: spiral turbulence

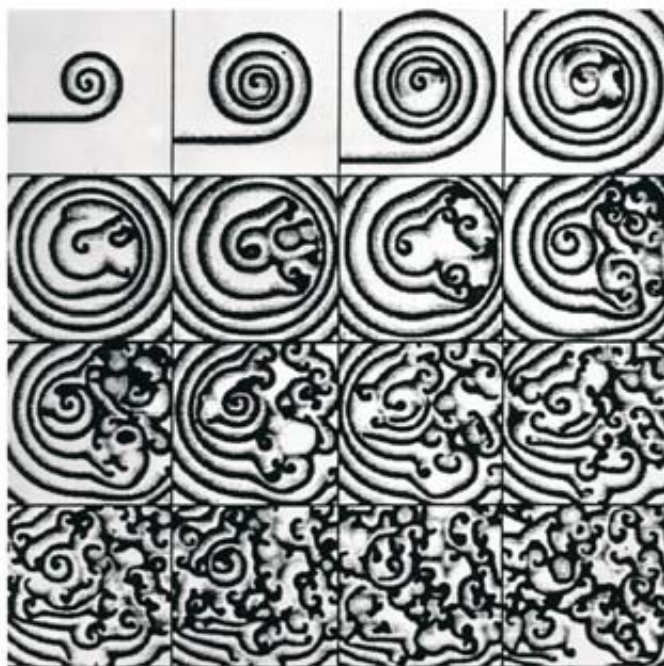


Figure 24. Computer simulation of the break-up of spiral waves to chemical turbulence.

## Chemical turbulence



Photoemission electron microscope (PEEM) imaging. Dark regions are predominantly oxygen covered, bright regions are mainly CO covered.

Real time, image size  $360 \times 360 \mu\text{m}$

Temperature  $T = 548 \text{ K}$ , oxygen partial pressure  $p_{\text{O}_2} = 4 \times 10^{-4} \text{ mbar}$ , CO partial pressure  $p_{\text{CO}} = 1.2 \times 10^{-4} \text{ mbar}$ .

Figure 25. PEEM image from a Pt(110) surface in the state of chemical turbulence.

We reached now a state where a system which in principle is very simple (a chemical reaction occurring between two diatomic molecules on a well-defined single crystal surface with fixed external parameters and for which all individual reaction steps are known) and which nevertheless exhibit rather complex behavior. Such effects are generally expected for open systems far



from equilibrium and are hence believed to govern also the whole nature. Our system can be considered to be a rather simple model for studying these types of phenomena. One might for example be interested to modify pattern formation from outside by affecting one of the control parameters. This can be done either locally by heating a small spot on the surface by laser light [50] or globally by a feedback mechanism in which the actual reaction rate (or integral coverage of one of the surface species) is used to regulate the flow of one of the reacting gases [51]. A series of patterns created in this way from a turbulent initial state by different strength and delay of the feedback is reproduced in fig. 26. These patterns are reminiscent of similar phenomena found in nature (fig. 27), but also on Vincent van Gogh's vision of our world in his painting "star night" (fig. 28).



Figure 26. Transformation of a state of spiral turbulence into different other patterns by a feedback mechanism with different strength and delay of the feedback [51].



Figure 27. Phenomena of pattern formation found in nature: The structure of the retina and leopard fur.



Figure 28. Vincent van Gogh's painting "Star night".

#### 4. CONCLUSIONS

This is no review article but a brief account for a broader audience of some of the work which had been considered to be the basis for the award. Numerous coworkers were involved in our continuing attempt to understand how chemical reactions on solid surfaces take place. Without their efforts the results presented could not have been achieved, and therefore I am heartily grateful to all of them. Their names as well as a complete bibliography up to 2004 can be found in a recent special issue of J. Phys. Chem. B [59].



## REFERENCES

- [1] J. Schiff (ed.) "Briefwechsel zwischen Goethe und Johann Wolfgang Döbereiner (1810 – 1830) (1994), 78. Published in: J. W. Döbereiner, Schweigg. J. 39 (1823) 1.
- [2] J. J. Berzelius, *Jber. Chem.* **15** (1835) 237 (submitted to the Academy on 31 March, 1835).
- [3] G. Ertl and T. Gloyna, *Z. Phys. Chem.* **217** (2003) 1207.
- [4] W. Ostwald, *Phys. Z.* **3** (1902) 313; *Ann. Naturphil.* **9** (1910) 1.
- [5] W. Crookes, Rep. of the 68<sup>th</sup> meeting of the British Association for the Advancement of Science, Bristol 1898. John Murray, London (1898), p. 3. Quoted after S. A. Topham, "Catalysis, Science and Technology" (eds. J. R. Anderson and M. Boudart), Springer Berlin, Vol. 7 (1955) p.1.
- [6] F. Haber, *Z. Elektrochem.* **16** (1910) 244; F. Haber and R. Le Rossignol, *Z. Elektrochem.* **19** (1913) 53.
- [7] W. Appl, "Ammonia", Wiley-VCH, Weinheim (1999).
- [8] A. Mittasch, "Geschichte der Ammoniak-Synthese", Verlag Chemie, Weinheim (1957).
- [9] P. H. Emmett, in "The physical basis for heterogeneous catalysis" (E. Drauglis and R. I. Jaffee, eds.), Plenum Press, New York (1975) p. 3.
- [10] G. Ertl, D. Prigge, R. Schlögl and D. Weiss, *J. Catal.* **79** (1983) 359.
- [11] I. Langmuir, *Trans. Faraday Soc.* **17** (1922) 607.
- [12] a) G. Ertl and J. Küppers, "Low energy electrons and surface chemistry", 2<sup>nd</sup> ed., VCH, Weinheim (1985). b) D. P. Woodruff and T. A. Delchar, "Modern techniques of surface science", Cambridge Univ. Press (1994). c) J. C. Vickerman, "Surface analysis: The principal techniques", Wiley (1997). d) K. W. Kolasinski, "Surface science. Foundations of catalysis and nanoscience", Wiley (2002).
- [13] J. E. Lennard-Jones, *Trans. Faraday Soc.* **28** (1932) 333.
- [14] a) G. Ertl, *Adv. Catalysis* **45** (2000) 1 b) A. C. Luntz, in "Chemical Bonding at Surfaces and Interfaces" (A. Nilsson, L. G. M. Pettersson, J. K. Nørskov, eds.), Elsevier 2008, p. 143.
- [15] J. Wintterlin, R. Schuster and G. Ertl, *Phys. Rev. Lett.* **77** (1996) 123.
- [16] G. Ertl, *J. Vac. Sci. Techn.* **14** (1977) 435.
- [17] a) S. Funk, M. Bonn, D. N. Denzler, Chr. Hess, M. Wolf and G. Ertl, *J. Chem. Phys.* **112** (2000) 9888. b) M. Bonn, S. Funk, C. Hess, D. N. Denzler, C. Stampfl, M. Scheffler, M. Wolf and G. Ertl, *Science* **285** (1999) 1042.
- [18] J. Wintterlin, J. Trost, S. Renisch, R. Schuster, T. Zambelli und G. Ertl, *Surface Sci.* **394** (1997) 159.
- [19] S. Renisch, R. Schuster, J. Wintterlin and G. Ertl, *Phys. Rev. Lett.* **82** (1999) 3839.
- [20] T. Zambelli, J. Trost, J. Wintterlin and G. Ertl, *Phys. Rev. Lett.* **76** (1996) 795.
- [21] R. Imbihl, R. J. Behm, G. Ertl and W. Moritz, *Surface Sci.* **123** (1982).
- [22] F. Boszo, G. Ertl, M. Grunze and M. Weiss, *J. Catal.* **49** (1977) 18; **50** (1977) 519.
- [23] a) G. Ertl, in "Encyclopedia of catalysis" (J. T. Hervath, E. Iglesia, M. T. Klein, J. A. Lercher, A. J. Russell and G. I. Stiefel, eds.) Wiley (2003) 1, 329. b) R. Schlögl, in "Handbook of heterogeneous catalysis", 2<sup>nd</sup> ed. (G. Ertl, H. Knözinger, F. Schüth and J. Weitkamp, eds.) Wiley-VCH (2008) ch. 12.1.
- [24] G. Ertl, M. Weiss and S. Lee, *Chem. Phys. Lett.* **60** (1979) 391.
- [25] N. D. Spencer, R. C. Schoonmaker and G. A. Somorjai, *J. Catal.* **74** (1982) 129.
- [26] G. Ertl, *Catal. Rev. Sci. Eng.* **21** (1980) 201.
- [27] P. Stoltze and J. K. Nørskov, *Phys. Rev. Lett.* **55** (1985) 2502; *J. Catal.* **110** (1998) 1.
- [28] a) M. Bowker, I. B. Parker and K. C. Waugh, *Appl. Cat.* **14** (1985) 101. b) J. A. Dumesic and A. A. Trevino, *J. Catal.* **116** (1989) 119. c) H. Topsoe, M. Boudart and J. K. Topsoe, eds, in "Topics in Catalysis", Vol.1 (1994).
- [29] S. Schwegmann, H. Over, V. De Renzi and G. Ertl, *Surface Sci.* **375** (1997) 91.
- [30] A. Föhlisch, M. Nyberg, J. Hasselström, O. Varis, L. G. M. Pettersson and A. Nilsson, *Phys. Rev. Lett.* **85** (2000) 3309.

- [31] a) C. N. Hinshelwood (Nobel Prize 1956), "The kinetics of chemical change", Clarendon Press, Oxford (1940). b) J. Wintterlin, S. Völkening, T. V. W. Janssens, T. Zambelli and G. Ertl, *Science* **278** (1997) 11931.
- [32] T. Kuri, P. Hu, T. Deutsch, P. L. Silvestrelli and J. Hutter, *Phys. Rev. Lett.* **80** (1998) 650.
- [33] a) P. Hugo, *Ber. Bunsenges.* **74** (1970) 121. b) H. Beusch, D. Fieguth and E. Wicke, *Chem. Ing. Techn.* **15** (1972) 445.
- [34] M. Eiswirth and G. Ertl, *Surface Sci.* **177** (1986) 90.
- [35] G. Nicolis and I. Prigogine, "Self-organization in non-equilibrium systems", Wiley (1977).
- [36] a) H. Haken, "Synergetics. An introduction" Springer (1977). b) A. S. Mikhailov, "Foundations of synergetics", Vol I and II, Springer (1991).
- [37] D. A. McLulich, "Variations in the number of varying hare" Univ. of Toronto Press, Toronto (193/) (after ref. [36a]).
- [38] I. Langmuir, *J. Am. Chem. Soc.* **38** (1916) 1221.
- [39] a) S. R. Bare, P. Hoffmann and D. A. King, *Surface Sci.* **144** (1984) 347. b) T. E. Jackman, J. A. Davies, D. P. Jackson, W. N. Unertl and P. R. Norton, *Surface Sci.* **120** (1982) 389.
- [40] T. Gritsch, D. Coulman, R. J. Behm and G. Ertl, *Phys. Rev. Lett.* **63** (1989) 1086.
- [41] N. Freyer, M. Kiskinova, D. Pirug and H. P. Bonzel, *Surface Sci.* **166** (1986) 206.
- [42] K. Krischer, M. Eiswirth and G. Ertl, *J. Chem. Phys.* **96** (1992) 9161.
- [43] M. M. Slinko and N. Jaeger, "Oscillating heterogeneous catalytic systems", Elsevier (1994).
- [44] F. Cirak, J. E. Cisternas, A. M. Cuitino, G. Ertl, P. Holmes, Y. Kevrekidis, M. Oritz, H. H. Rotermund, M. Schunack and J. Wolff, *Science* **300** (2003) 1932.
- [45] a) G. Ertl, *Science* **254** (1991) 1750. b) R. Imbihl and G. Ertl, *Chem. Rev.* **95** (1995) 697.
- [46] W. Engel, M. Kordesch, H. H. Rotermund, S. Kubala and A. von Oertzen, *Ultramicroscopy* **95** (1991) 6162.
- [47] S. Jakubith, H. H. Rotermund, W. Engel, A. von Oertzen and G. Ertl, *Phys. Rev. Lett.* **65** (1990) 3013.
- [48] S. Nettesheim, A. von Oertzen, H. H. Rotermund and G. Ertl, *J. Chem. Phys.* **98** (1993) 9977.
- [49] M. Bär, N. Gottschalk, M. Eiswirth and G. Ertl, *J. Chem. Phys.* **100** (1994) 1202.
- [50] J. Wolff, A. G. Papathanasiou, Y. Kevrekidis, H. H. Rotermund and G. Ertl, *Science* **294** (2001) 134.
- [51] M. Kim, M. Bertram, M. Pollmann, A. von Oertzen, A. S. Mikhailov, H. H. Rotermund and G. Ertl, *Science* **292** (2001) 1357.
- [52] *J. Phys. Chem. B* **108** (2004), pp. 14183-14788.

Portrait photo of Gerhard Ertl by photographer Ulla Montan.